Journal of Alloys and Compounds 729 (2017) 730–734

Contents lists available at ScienceDirect

Journal of Alloys and Compounds

journal homepage: http://www.elsevier.com/locate/jalcom

Microstructure refinement and magnetization improvement in CoFe thin films by high magnetic field annealing

Hanlu Zhang [a, b], Xianwu Tang [a, **], Renhuai Wei [a], Shunjin Zhu [a], Jie Yang [a], Wenhai Song [a], Jianming Dai [a], Xuebin Zhu [a, *], Yuping Sun [a, c]

[a] Key Laboratory of Materials Physics, Institute of Solid State Physics, Chinese Academy of Sciences, Hefei 230031, People's Republic of China
[b] University of Science and Technology of China, Hefei 230026, People's Republic of China
[c] High Magnetic Field Laboratory, Chinese Academy of Sciences, Hefei 230031, People's Republic of China

ARTICLE INFO

Article history:
Received 27 March 2017
Received in revised form
20 September 2017
Accepted 21 September 2017
Available online 22 September 2017

Keywords:
Magnetic field annealing
CoFe
Thin films
Ferromagnetism
Chemical solution deposition

ABSTRACT

Co-Fe alloy thin films with high magnetization are desirable in numerous applications. Co-Fe thin films prepared by solution methods with refined microstructures have not been achieved up to now. Here, high magnetic field annealing (HMFA) is introduced for the preparation of $Co_{70}Fe_{30}$ alloy thin films. The effects of HMFA on their microstructures and room temperature magnetic properties are investigated. The thickness of the derived $Co_{70}Fe_{30}$ thin films is dramatically decreased from a value of 590 nm without HMFA to 320 nm with 7 T magnetic field annealing, and the refinement of microstructures is also observed with HMFA. The derived $Co_{70}Fe_{30}$ film annealed under 7 T magnetic field exhibits a saturation magnetization of ~2.43 T, close to the theoretical value of 2.45 T. Overall, HMFA provides a feasible way to fabricate larger-area and denser Co-Fe thin films with excellent magnetic properties.

1. Introduction

As an important type of transition metal alloy, CoFe binary alloys show excellent soft magnetic properties, including high saturation magnetization, low coercivity, high permeability, good thermal stability, and giant magnetostriction [1–6]. Hence, CoFe-based nanoparticles and thin films are considered as promising candidates for a number of applications in the fields of magnetic data storage, nanocomposite permanent magnets, high frequency apparatus, catalysts, etc [7,8]. Additionally, as one type of electromagnetic wave absorption material, the main absorption band and intensity can be obviously controlled by varying the Co/Fe molecular ratio and the microstructures [9,10]. Currently, various methods, including both physical and chemical routes, have been used to prepare CoFe alloy thin films [1,11–16]. Compared with the physical methods, the chemical solution methods have several advantages, such as low-cost, large-scale fabrication, and easy control from the view-point of applications [17]. Nevertheless, CoFe alloy thin films derived by chemical solution methods such as electrodeposition usually show loose and/or porous microstructures, resulting in low magnetization [18–20]. To improve the performances of CoFe alloy thin films, it is crucial to improve the thin film density. The common route to enhancing density is to increase the grain size by prolonging the dwell time during annealing or increasing the annealing temperature, although the applications of CoFe alloys with large grain size are limited. Thus, it is very vital to prepare CoFe alloy thin films with refined microstructures by solution methods to make them suitable for a wide range of applications.

Previous theoretical calculations have suggested that high magnetic field annealing (HMFA) can strongly affect the microstructure as well as the magnetic properties of Co-Fe alloys [21]. Experimentally, low magnetic field (no more than 1 T) annealing has been used to improve the microstructures and properties of electrodeposited CoFe alloys thin films in recent years. In CoFe thin films, a changed structure and an enhanced deposition mass are observed when they are fabricated by an electrochemical method in an applied field of 500 mT [22]. An increased compressive stress was induced in $Co_{0.3}Fe_{0.7}$ thin films by post-deposition field-annealing in 100 Oe from 100 to 400 °C [23]. With 10 kOe magnetic field annealing, FeCo films achieved desirable, thermally stable

* Corresponding author.
** Corresponding author.
E-mail addresses: xwtang@issp.ac.cn (X. Tang), xbzhu@issp.ac.cn (X. Zhu).

https://doi.org/10.1016/j.jallcom.2017.09.227
0925-8388/

properties for high frequency functions [17]. Due to the low applied magnetic fields, however, investigations of the magnetic annealing effects have been limited. Thus, a further investigation of HMFA effects on the grain growth, the microstructures, and the magnetic properties of CoFe alloys thin films is desirable.

In this work, polycrystalline $Co_{70}Fe_{30}$ (CF) thin films have been prepared by chemical solution deposition on yttrium stabilized zirconia (YSZ) substrates. The HMFA effects on the grain growth, the microstructures, and the magnetic properties of the thin films are investigated. Due to the enhancement of nucleation and the extra grain growth force induced by the magnetic field, the grain growth rate is enhanced, resulting in variation of the microstructures for the derived thin films. CoFe thin films with refined microstructures, enhanced thin film density, and high saturation magnetization close to the theoretical value can be prepared by HMFA processing.

2. Experiment

The amorphous CF thin films were deposited on the YSZ single crystal substrates by chemical solution deposition (CSD). The CF precursor solution with a concentration of 0.01 M was prepared from cobalt (II) acetate anhydrous and iron (III) nitrate nonahydrate as precursor salts, and 2-methoxyethanol as a solvent. The precursor was spin-coated onto the YSZ substrates with a rotation rate of 5000 rpm for 10 s, and then baked at 150 °C for 2 min. A further pyrolysis treatment at 400 °C for 10 min in air was carried out to remove the organic residues. To enhance the film thickness, the above processing was repeated eight times. Finally, each thin film was annealed at 700 °C in a forming gas (ratio of N_2:H_2 4:1 v/v) for 60 min under magnetic fields of 0, 1, 3, 5, or 7 T, where the magnetic field was parallel to the thin film surface. In the annealing processing, the precursor network collapses, and the final CoFe phase will nucleate and grow, resulting in different thin film thickness. Due to the high magnetic field effects on the increased nucleation and grain growth, the collapse of the precursor network is more severe, and the thin films become denser, which leads to the decrease in thin film thickness under the HMFA processing. The derived thin films at each corresponding magnetic field (in Tesla) are respectively labeled as CF0, CF1, CF3, CF5, and CF7. Glancing angle X-ray diffraction (XRD) was performed with monochromatic Cu K_α radiation on an X'pert Pro machine (PANalytical B. V., Almelo, Netherlands) to investigate the phase and quality of the derived thin films. The surface morphology and thickness were determined using a field-emission scanning electron microscope (FE-SEM, SU8020, Hitachi, Japan). The in-plane microstructure was characterized by a transmission electron microscope (TEM, JEM-2010, JEOL, Japan). Magnetic properties at room temperature were measured with a superconducting quantum interference device (SQUID) (MPMS XL5, Quantum Designed, USA).

3. Results and discussion

The glancing angle XRD patterns of the derived CoFe (CF) thin films annealed under different high magnetic fields are shown in Fig. 1. All the diffraction peaks match well with the pattern of bulk body-centered cubic $Co_{70}Fe_{30}$ (JCPDS 048-1818), which well agree with the reference data [24]. Notably, all thin films exhibit a strong (110) diffraction peak and two weak diffraction peaks, suggesting the polycrystalline nature of the as-prepared CF thin films. The lattice constant of all the derived CF alloy films is approximately 0.284 nm, which is similar to that of the electrodeposited CF [25] and shows no changes with increasing the magnetic field. The average crystallite size was estimated by the Scherrer Equation, and the results are shown in the inset table of Fig. 1. As shown in the table, the average crystallite size decreases initially and then

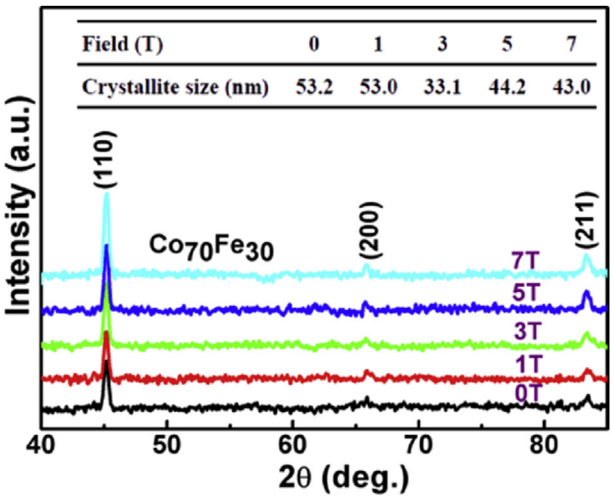

Fig. 1. Glancing XRD patterns for the CF thin films annealed under different high magnetic fields. The average crystallite size is listed in the inset table.

increases with increasing magnetic field. The initial decrease in the crystallite size with increasing magnetic field indicates that high magnetic fields can affect the CF thin film nucleation. The following increased crystallite size with further increase in the magnetic field suggests that the grain growth is obviously affected by the applied magnetic field.

Surface and cross-sectional FE-SEM images of the as-prepared CF thin films annealed under different high magnetic fields are shown in Fig. 2(a–e) and (f–k), respectively. Usually, the thin film particle size, with each particle containing several crystallites, as shown in Fig. 2(a–e), decreases initially and then increases with increasing magnetic field. The variation in the particle size corroborates the results shown in the inset table of Fig. 1. Additionally, some pores exist in the thin film CF0 without HMFA, as shown in Fig. 2(a), which may be caused by the removal of the organic residues at high annealing temperature. Interestingly, the pores are notably reduced under low magnetic field annealing (LMFA) and even eliminated under HMFA. Additionally, in the case of the CF thin films annealed under higher magnetic fields, some much larger particles are observed, as shown in Fig. 2(d) and (e), indicating the existence of abnormal grain growth [26]. The occurrence of abnormal grain growth suggests that a compressive strain is always induced during the CF thin film grain growth. In contrast, as shown in Fig. 2(f–k), the thickness of the prepared CF alloy thin films decreases from 590 nm for the CF0 film to 320 nm for the thin CF7 film. The obvious reduction in thickness indicates that thin film density increases with HMFA. During the processing, the magnetic field can enhance the nucleation rate and the grain growth rate, which leads to the changes in the grain size and particle size. Due to the enhancement of nucleation and grain growth, the pores in the thin films will be reduced, resulting in denser and thinner thin films. Thus, the loose CF alloy thin films can be drastically densified by HMFA processing.

To further investigate the HMFA effects on the microstructure and the surface morphology of the thin films, TEM observations of the derived CF0 and CF5 thin films were carried out, and the results are shown in Fig. 3. The selected area electron diffraction (SAED) pattern of the CF0 film and the high-resolution TEM (HRTEM) image of the CF5 thin film are displayed in the corresponding insets of Fig. 3. The clearer and sharper inner reflections, as shown in the SAED pattern, imply better crystallization and a body-centered cubic structure for the derived CF thin films. Clear lattice strips with lattice fringe spacing values close to the bulk lattice constant

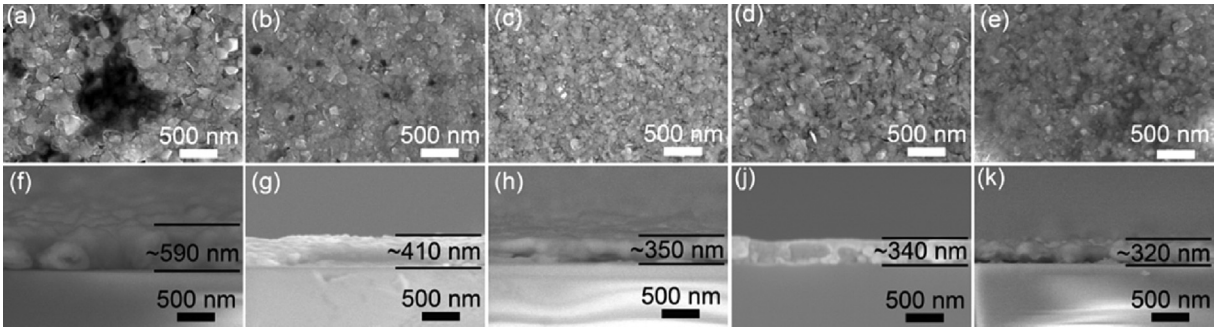

Fig. 2. FE-SEM images of the derived CF thin films: (a) CF0, (b) CF1, (c) CF3, (d) CF5, and (e) CF7. Cross-sectional FE-SEM images of the films: (f) CF0, (g) CF1, (h) CF3, (j) CF5, and (k) CF7.

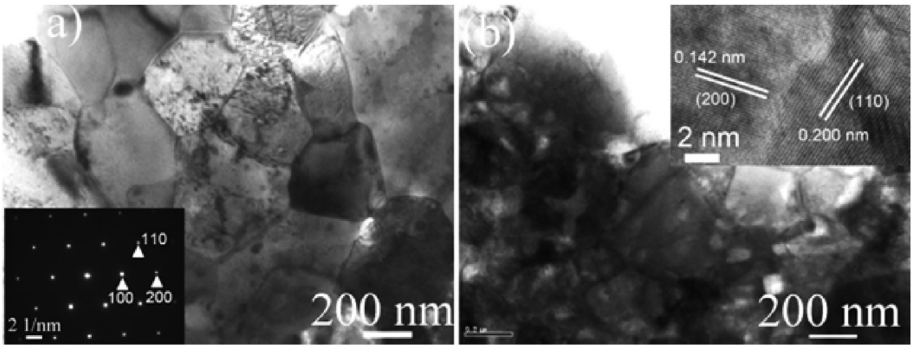

Fig. 3. Cross-sectional TEM images of CF thin films: (a) CF0, and (b) CF5. The selected area electron diffraction pattern for the CF0 film and a high-resolution TEM image of the CF5 film are respectively displayed as insets to (a) and (b).

are displayed in the inset of Fig. 3(b) for the CF5 thin film, which is the same as the results derived from the XRD patterns. Additionally, the CF5 thin film shows a smaller grain size with blurred grain boundaries as compared to the CF0 thin film, which agree with the results shown in the inset table of Fig. 1 and in Fig. 2. These results further confirm that the application of magnetic field in thin film preparation can affect the nucleation and the grain growth. Additionally, the average crystallite size derived from the XRD results and the TEM observations is almost the same.

To summarize, we assume that, the above-mentioned modified microstructures of the derived CF thin films with reduced pores and enhanced density should be formed as a result of the increased nucleation and the enhanced grain growth with HMFA processing. According to the nucleation theory [27], the steady-state homogeneous nucleation rate I_{st} can be described as follows

$$I_{st} = I_0 \cdot \exp\left(-\frac{Q}{RT}\right) \cdot \exp\left(-\frac{\Delta G_c}{RT}\right),$$

where I_0 is the pre-exponential factor, Q represents the activation energy, R is the universal gas constant, T is the absolute temperature, and ΔG_c is the Gibbs free energy required to form a critical sized nucleus. It can be deduced that the larger ΔG_c is, the more nuclei will be produced. Furthermore, due to the effect of the magnetic energy originating from a static magnetic field, the nucleation rate can be rewritten as [28]

$$I_{st} = I_0 \cdot \exp\left(-\frac{Q}{RT}\right) \cdot \exp\left(\frac{-\Delta G_c + \Delta G_H}{RT}\right),$$

where ΔG_H is the magnetic field induced difference in the free energy. Here ΔG_H can be described as [28]: $\Delta G_H = -\mu_0 \cdot \Delta M(T) \cdot H - \frac{1}{2}\Delta\chi H^2$, where μ_0 is the permeability in vacuum, $\Delta M(T)$ and $\Delta\chi$ are the respective differences in the magnetization and magnetic susceptibility between the crystalline and the amorphous phase, and H is the applied magnetic field intensity. In present study, all the derived CF thin films were crystallized from pyrolyzed thin films composed of Fe- and Co-containing precursors, which have much lower magnetization and susceptibility as compared with those of the bulk crystallized CF alloys. Therefore, much larger values of $\Delta M(T)$ and $\Delta\chi$ will be produced under a high magnetic field, leading to a lower ΔG_H and a larger I_{st}, as well as more nuclei, during the HMFA processing. Compared with the effects of high annealing temperature, the much lower ΔG_H caused by low applied magnetic fields will have a little effect on the I_{st}, resulting in a small change in the crystallite size, as shown in Table 1. On increasing the magnetic field, the enhanced magnetic energy will cause an unavoidable effect on the thin film I_{st}, leading to a more pronounced nucleation and resulting in a small crystallite size [26]. The increased crystallite size on further increasing the magnetic field, as shown in the inset table of Fig. 1, may be attributed to the enhanced magnetic force, which acts as an extra growth factor induced by the magnetic field. Besides the magnetic energy induced by the applied magnetic field, the enhanced magnetic force with increasing magnetic field acts as an extra growth force (p), as described by an equation $p = \frac{1}{2}\Delta\chi H^2$ [29], that will accelerate the movement of the grain boundaries. As a result, the crystallite size of the thin film will increase with increasing applied magnetic field, causing a larger crystallite size in the thin films CF5 and CF7.

Room temperature hysteresis loops (M-H) are measured by applying magnetic fields that are perpendicular (out-of-plane) and parallel (in-plane) to the thin film surfaces. The measured in-plane (IP) and out-of-plane (OP) M-H loops of all the prepared thin films

Table 1
Comparison of room temperature IP and OP magnetic properties of the derived films, including M_s, M_r, M_s^{pa}, M_r^{pa}, SQR, and H_C.

Field	IP					OP				
	0	1	3	5	7	0	1	3	5	7
M_s (emu/cm^3)	1024	1340	1833	1911	1936	450	820	1008	1046	1073
M_r (emu/cm^3)	620	890	1280	1300	1340	112	290	227	304	371
M_s^{pa} (emu/cm^2)	60.42	54.94	64.16	66.89	65.82	26.55	33.62	35.28	36.61	36.48
M_r^{pa} (emu/cm^2)	36.58	36.49	44.80	45.50	45.56	6.61	11.89	7.95	10.64	12.61
SQR	0.61	0.66	0.70	0.68	0.69	0.25	0.35	0.23	0.29	0.35
H_C (Oe)	74	65	60	53	42	75	96	76	51	70

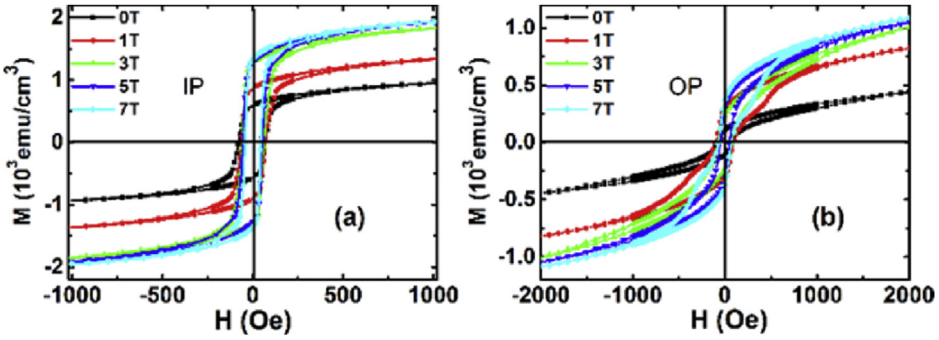

Fig. 4. In-plane (IP) (a) and out-of-plane (OP) (b) hysteresis loops of the CF thin films annealed under different high magnetic fields.

are shown in Fig. 4(a) and (b), respectively. The different shapes of the loops for the IP and OP *M-H* curves are attributed to the magnetic anisotropy, with an IP being an easy axis and an OP presenting a hard one, which agrees with the reference data [18]. To give a clear picture of the HMFA effects on the thin film magnetic properties, the saturation magnetization M_s (defined as the magnetization at the maximum applied magnetic field), the coercivity field (H_C), the remanent magnetization (M_r), and the remanence ratio (SQR, defined as M_r/M_s) were determined from the room temperature *M-H* loops and are listed in Table 1. Most of the values of M_s are over 1000 emu/cm^3 for both the IP and the OP directions. In particular, the IP M_s value of the CF7 thin film reaches as high as 1936 emu/cm^3 (~2.43 T), which is very close to the theoretical value of 2.45 T [3]. In addition, as shown in Table 1, both the M_s and the M_r increase monotonically as the annealing magnetic field increases for both the IP and the OP directions. Generally, an enhancement in grain size will lead to an increased magnetization [23]. For the as-prepared CF films, however, the crystallite/particle size, as shown in Fig. 1 or Fig. 2, does not increase with increasing applied magnetic field. Meanwhile, the CF thin film thickness does decrease with increasing applied magnetic field, as shown in Fig. 2(f–k). To avoid the influence of the thin film thickness on the calculated magnetization value due to the difference in density, the saturation magnetization per unit area (M_s^{pa}) and the remanent magnetization per unit area (M_r^{pa}) were calculated and are listed in Table 1. Clearly, both M_s^{pa} and M_r^{pa} decrease initially and then increase with increasing annealing magnetic field, which is a result of the variation in crystallite/grain size, as mentioned above. The magnetization per area of the CF thin films prepared using HMFA processing, such as CF3, CF5, and CF7, is larger than that of the CF0 thin film, and these films have a smaller crystalline size. The results suggest that HMFA processing can improve the magnetic properties of the solution-derived CF thin films. In the case of the M_s, such increased magnetization may be caused by the decreased concentration of the defects, including pores and disordered grain boundaries, as well as the enhanced alignment of magnetic moments due to the increased magnetic field. The pores caused by the rapid decomposition of organic compounds during preparation are unavoidable, which will lead to low thin film density. The magnetization of a magnetic thin film is presented in units of magnetic moment per unit volume. The decreased concentration of pores will lead to a decrease in volume, resulting in increased magnetization of the thin film. To avoid ambiguity, the saturation magnetization is defined as the thin film magnetization in the largest applied magnetic field. In the calculation of the saturation magnetization for the thin films, the volume of the thin film influences this value to a certain extent. So, the decreased in a number of the defects such as pores would densify the thin films and decrease the volume of the thin films, which effectively improves the value of the saturation magnetization. At the same time, the grain shape anisotropy may also make some contribution to the varied magnetization [30].

In the case of the remanence ratio, the IP SQR value initially increases and then decreases slightly, while the OP one shows the opposite trend with increasing annealing magnetic field. Since the annealing temperature is 700 °C, which is below the Curie temperature of the CF alloy (~ 920 °C) [3], the IP directional uniaxial magnetic anisotropy in the thin films cannot be ignored for the parallel annealing magnetic field [12]. Thus, the increased IP SQR may be attributed to the increase in the uniaxial magnetic anisotropy as the annealing magnetic field increases. The resulting slightly decreased IP SQR on further increasing the annealing magnetic field may be caused by a compressive strain relaxation in the thin film due to abnormal grain growth, as shown in Fig. 2. In the case of the OP SQR, the initial variations may originate from the reduction in pores and the decrease in cubic anisotropy caused by the refined grains. The following increased IP and OP SQR values may be related to the enlarged crystallite size and the decreased tensile strain in the OP direction resulting from the relaxed compressive strain in the IP direction.

As shown in Table 1, the IP H_C decreases monotonically, while the OP H_C behaves in an irregular way as the high magnetic field during the annealing process is further increased. At the same time, this also indicates that the applied parallel annealing magnetic field

plays an important role in the IP directional magnetization reversal of the CF thin films. Along with the thin film microstructures, the initial decrease in the IP H_C can be caused by the decreased number of pores, as shown in Fig. 2. With further increase of the annealing magnetic field, the reduced H_C can be attributed to the decreased number of grain boundaries and blurred grain boundaries resulting from the grain growth in HMFA processing. Additionally, the relaxation of the thin film strain also makes a contribution to the reduced IP H_C.

4. Conclusion

In summary, high magnetic field annealing effects the microstructure and the room temperature magnetic properties of $Co_{70}Fe_{30}$ alloy thin films. The crystallite size/grain size initially decreases and then increases with increasing magnetic field, with the decrease and increase attributed respectively to the increase in nucleation and the extra grain growth force induced by the applied magnetic field. The magnetic properties are improved, including increased saturation and remanence magnetization, and a larger remanence ratio, as well as softened coercivity. Especially, the CF thin film annealed under 7 T magnetic field exhibits a saturation magnetization of 2.43 T, which is close to the theoretical value of 2.45 T. The improved magnetic properties can be attributed to the optimized grain growth and the modified microstructure in the CF thin films due to HMFA processing. These results will provide an effective route to the fabrication of high magnetization Co-Fe alloys thin films with significantly improved density, through using solution methods for large-area applications.

Acknowledgements

This work was supported by the National Natural Science Foundation of China (NSFC, Nos. 11204316 and 11374304), the Joint Funds of the National NSFC and the Chinese Academy of Sciences (CAS) Large-Scale Scientific Facility (Nos. U1432137 and U1232210). Thanks to Dr. Tania M. Sliver of University of Wollongong for English improvement.

References

[1] D. Hunter, W. Osborn, K. Wang, N. Kazantseva, J. Hattrick-Simpers, R. Suchoski, R. Takahashi, M.L. Young, A. Mehta, L.A. Bendersky, S.E. Lofland, M. Wuttig, I. Takeuchi, Giant magnetostriction in annealed $Co_{1-x}Fe_x$ thin-films, Nat. Commun. 2 (2011) 518.
[2] G. Scheunert, O. Heinonen, R. Hardeman, A. Lapicki, M. Gubbins, R.M. Bowman, A review of high magnetic moment thin films for microscale and nanotechnology applications, Appl. Phys. Rev. 3 (2016) 011301.
[3] R.S. Sunder, S.C. Deevi, Soft magnetic FeCo alloys: alloy development, processing, and properties, Int. Mater. Rev. 50 (2005) 157–192.
[4] N. Ishiwata, C. Wakabayashi, H. Urai, Soft magnetism of high-nitrogen-concentration FeTaN films, J. Appl. Phys. 69 (1991) 5616–5618.
[5] S. Ohnuma, N. Kobayashi, T. Masumoto, S. Mitani, H. Fujimori, Magnetostriction and soft magnetic properties of $(Co_{1-x}Fe_x)$-Al-O granular films with high electrical resistivity, J. Appl. Phys. 85 (1999) 4574–4576.
[6] S. Ikeda, I. Tagawa, Y. Uehara, T. Kubomiya, J. Kane, M. Kakehi, A. Chikazawa, Write heads with pole tip consisting of high-B_s FeCoAlO films, IEEE Trans. Magn. 38 (2002) 2219–2221.
[7] H. Chang, H. Chen, Z. Shao, J. Shi, J. Bai, S.D. Li, In situ fabrication of $(Sr,La)FeO_4$ with CoFe alloy nanoparticles as an independent catalyst layer for direct methane-based solid oxide fuel cells with a nickel cermet anode, J. Mater. Chem. A 4 (2016) 13997–14007.
[8] P. Cai, Y. Hong, S. Ci, Z. Wen, In situ integration of CoFe alloy nanoparticles with nitrogen-doped carbon nanotubes as advanced bifunctional cathode catalysts for Zn–air batteries, Nanoscale 8 (2016) 20048–20055.
[9] Y. Yang, C. Xu, Y. Xia, T. Wang, F. Li, Synthesis and microwave absorption properties of FeCo nanoplates, J. Alloys Compd. 493 (2010) 549–552.
[10] Z.X. Yu, N. Zhang, Z.P. Yao, X.J. Han, Z.H. Jiang, Synthesis of hierarchical dendritic micro-nano structure Co_xFe_{1-x} alloy with tunable electromagnetic absorption performance, J. Mater. Chem. A 1 (2013) 12462–12470.
[11] T.H. Kim, Y.H. Jeong, J.S. Kang, Structural and magnetic properties of CoFe alloy films, J. Appl. Phys. 81 (1997) 4764–4766.
[12] T. Nakajima, T. Takeuchi, I. Yuito, K. Kato, M. Saito, K. Abe, T. Sasaki, T. Sekiguchi, S. Yamaura, Effect of annealing on magnetostrictive properties of FeCo alloy thin films, Mater. Trans. 55 (2014) 556–560.
[13] C.X. Ji, F. Lu, Y.A. Chang, J.J. Yang, M.S. Rzchowski, Growth and physical property of epitaxial $Co_{70}Fe_{30}$ thin film on Si substrate via TiN buffer, Appl. Phys. Lett. 92 (2008) 022504.
[14] A.T. Hindmarch, D.A. Arena, K.J. Dempsey, M. Henini, C.H. Marrows, Influence of deposition field on the magnetic anisotropy in epitaxial $Co_{70}Fe_{30}$ films on GaAs(001), Phys. Rev. B 81 (2010) 100407(R).
[15] G.K. Rajan, S. Ramaswamy, C. Gopalakrishnan, D.J. Thiruvadiga, Effect of an external magnetic field on the morphology and magnetic properties of CoFe nanostructures, Phys. Status Solidi A 208 (2011) 2847–2852.
[16] T. Osaka, T. Yokoshima, D. Shiga, K. Imai, K. Takashima, A high moment CoFe soft magnetic thin film prepared by electrodeposition, Electrochem. Solid State Lett. 6 (2003) C53–C55.
[17] B.Y. Zong, N.N. Phuoc, Y.P. Wu, P. Ho, Y. Yang, Z.W. Li, Electrodeposited thin FeCo films with highly thermal stable properties in high frequency range obtained by annealing in a strong magnetic field, J. Appl. Phys. 120 (2016) 065306.
[18] M. del C. Aguirre, E. Farías, J. Abraham, S.E. Urreta, $Co_{100-x}Fe_x$ magnetic thick films prepared by electrodeposition, J. Alloys Compd. 627 (2015) 393–401.
[19] D. Kim, D.Y. Park, B.Y. Yoo, P.T.A. Sumodjo, N.V. Myung, Magnetic properties of nanocrystalline iron group thin film alloys electrodeposited from sulfate and chloride baths, Electrochim. Acta 48 (2003) 819–830.
[20] L. Ricq, F. Lallemand, M.P. Gigandet, J Pagetti, Influence of sodium saccharin on the electrodeposition and characterization of CoFe magnetic film, Surf. Coat. Technol. 138 (2001) 278–283.
[21] Y. Hanlumyuang, P.R. Ohodnicki, A.D.E. Laughlin, M.E. McHenry, Bragg-Williams model of Fe-Co order-disorder phase transformations in a strong magnetic field, J. Appl. Phys. 99 (2006) 08F101.
[22] F. Karnbach, M. Uhlemann, A. Gebert, J. Eckert, K. Tschulik, Magnetic field templated patterning of the soft magnetic alloy CoFe, Electrochim. Acta 123 (2014) 477–484.
[23] L.X. Phua, N.N. Phuoc, C.K. Ong, Influence of field-annealing on the microstructure, magnetic and microwave properties of electrodeposited $Co_{0.3}Fe_{0.7}$ films, J. Alloys Compd. 553 (2013) 146–151.
[24] Y. Han, H. Wang, T. Zhang, Y. He, J.M.D. Coey, C. Jiang, Tailoring the heterogeneous magnetostriction in Fe-Co alloys, J. Alloys Compd. 699 (2017) 200–209.
[25] C.V. Thompson, Structure evolution during processing of polycrystalline films, Annu. Rev. Mater. Sci. 30 (2000) 159–190.
[26] K. Lu, Nanocrystalline metals crystallized from amorphous solids: nanocrystallization, structure, and properties, Mater. Sci. Eng. R 16 (1996) 161–221.
[27] B.Z. Cui, K. Han, H. Garmestani, J.H. Su, H.J. Schneider-Muntau, J.P. Liu, Enhancement of exchange coupling and hard magnetic properties in nanocomposites by magnetic annealing, Acta Mater. 53 (2005) 4155–4161.
[28] T. Kakeshita, T. Saburi, K. Shimizu, Effects of hydrostatic pressure and magnetic field on martensitic transformations, Mater. Sci. Eng. A 273–275 (1999) 21–39.
[29] D.A. Molodov, A.D. Sheikh-Ali, Effect of magnetic field on texture evolution in titanium, Acta Mater. 52 (2004) 4377–4383.
[30] N.A. Frey, S. Peng, K. Cheng, S.H. Sun, Magnetic nanoparticles: synthesis, functionalization, and applications in bioimaging and magnetic energy storage, Chem. Soc. Rev. 38 (2009) 2532–2542.